

PdH_x Entrapped in a Covalent Triazine Framework Modulates Selectivity in Glycerol Oxidation

Carine E. Chan-Thaw,^[a] Alberto Villa,^[a] Di Wang,^[b] Vladimiro Dal Santo,^[c]
Alessio Orbelli Biroli,^[c] Gabriel M. Veith,^[d] Arne Thomas,^[e] and Laura Prati^{*[a]}

Pd nanoparticles within a nitrogen-containing covalent triazine framework (CTF) material are investigated to understand if the highly tunable CTF chemistry mediates the catalytic properties of the Pd nanoparticles. Surprisingly, our results demonstrate that the CTF stabilizes the formation of 2.6 nm PdH_x particles within the pores. These confined PdH_x particles are very active for the liquid-phase oxidation of glycerol and promote C–C cleavage, probably connected with the enhanced in situ forma-

tion of H₂O₂. During recycling tests, the confined particles are transformed progressively to very stable Pd⁰ particles. This stability has been attributed mainly to a confinement effect as nanoparticles trapped outside the pores lose activity rapidly. These results indicate that there is a potential to tune CTF chemistry to modify the chemistry of the catalytic metals significantly.

Introduction

In this work, we demonstrate that a covalent triazine framework (CTF) is able to stabilize the in situ formation of PdH_x particles, which mediate the activity and selectivity of this catalyst directly for the liquid-phase oxidation of glycerol. Moreover, we validated the role of nascent H₂O₂ towards C–C cleavage experimentally, which provides a new way to tune the chemical reactivity of these catalysts.

CTFs are produced by the ionothermal trimerization of carbonitrile groups (*p*-dicyanobenzene) in molten ZnCl₂, which acts as both catalyst and solvent at temperatures of 400–600 °C.^[1] At this latter temperature, a dynamic reorganization of the porous polymer networks takes place. Therefore, CTFs exhibit very high surface areas and high amounts of nitrogen

functionalities in the network. As a result of their fully covalent structure, they possess an increased thermal and chemical stability. CTFs have been used as the support for metal nanoparticles (NPs) in catalysis.^[2] Indeed, we reported previously that the N heteroatoms within a CTF stabilize PdNPs protected by polyvinylalcohol (PVA; Pd_{PVA}/CTF) during alcohol oxidation better than activated carbon (Pd_{PVA}/AC).^[2b-d] Indeed, during the liquid-phase oxidation of glycerol, Pd_{PVA}/AC deactivates immediately in the first run; whereas the same NPs supported on CTF (Pd_{PVA}/CTF) exhibited stable catalytic activity over three cycles. This result is important because it is particularly challenging to design and prepare selective and robust catalysts for liquid-phase reactions that avoid common problems of particle migration, coarsening, leaching, or modification of the catalyst support structure.^[3] To further increase the stability of Pd/CTF, we investigated the impact of a preparation technique, namely impregnation (IMP), that would lead to the confinement of the particles of Pd within the pores of the CTF (Pd_{IMP}). This confinement should result in a new chemical “dial” to control material properties and tune reactivity.

Results and Discussion

The TEM overview image of Pd_{IMP}/CTF shows that the PdNPs were ≈2.6 nm in size (Table 1, Figure 1b), in close agreement with the mean pore size of CTF determined by nitrogen adsorption (2.7 nm).^[4] Conversely, the use of the sol-immobiliza-

[a] Dr. C. E. Chan-Thaw, Dr. A. Villa, Prof. L. Prati
Department of Chemistry
Università degli Studi di Milano
via Golgi 19, 20133 Milano (Italy)
E-mail: laura.prati@unimi.it

[b] Dr. D. Wang
Institute of Nanotechnology and Karlsruhe Nano Micro Facility
Karlsruhe institute of technology (KIT)
Hermann-von-Helmholtz-Platz 1, 76344
Eggenstein-Leopoldshafen (Germany)

[c] Dr. V. D. Santo, Dr. A. Orbelli Biroli
CNR-Istituto di Scienze e Tecnologie Molecolari
Via C. Golgi 19, 20133 Milano (Italy)

[d] Dr. G. M. Veith
Materials Science and Technology Division
Oak Ridge National Laboratory
Oak Ridge, TN 37831 (USA)

[e] Prof. A. Thomas
Department of Chemistry, Functional Materials
Technische Universität Berlin
Hardenbergstr. 40, 10623 Berlin (Germany)

This publication is part of a Special Issue on Palladium Catalysis. To view the complete issue, visit:
<http://onlinelibrary.wiley.com/doi/10.1002/cctc.v7.14/issuetoc>

Table 1. Mean PdNPs dimensions determined by TEM.

	Statistical median [nm]	Standard deviation σ
Pd _{PVA} /CTF	3.1	0.7
Pd _{IMP} /CTF	2.6	0.6

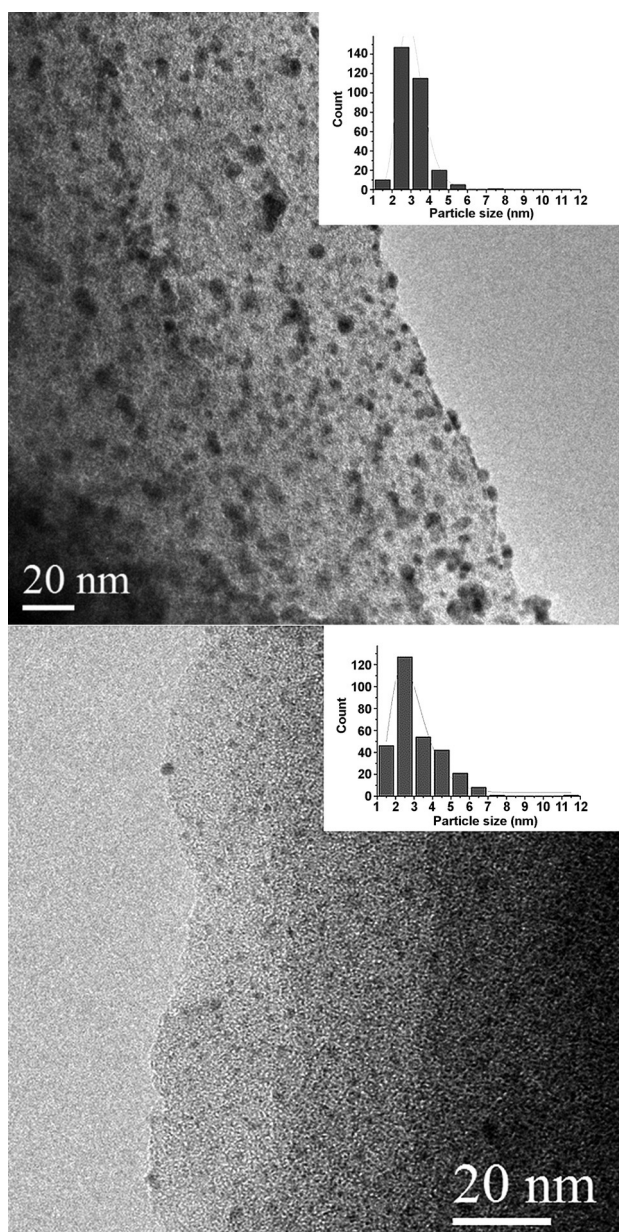


Figure 1. TEM images of a) Pd_{PVA}/CTF and b) Pd_{IMP}/CTF.

tion technique (Pd_{PVA}/CTF) led to a PdNP size of 3.1 nm, which depends on the preformed metallic sol (Table 1, Figure 1 a).

Pd X-ray photoelectron spectroscopy (XPS) revealed a 93% reduction in Pd intensity of the Pd_{IMP} sample compared to that of the Pd_{PVA} material despite the identical 1 wt% metal loadings (XPS signal = 3.0 at% Pd for Pd_{PVA}/CTF; 0.2 at% Pd for Pd_{IMP}/CTF; Table 2). The high dispersion and narrow distribution of the Pd particle size with the lack of large Pd particles evidenced by microscopy (Figure 1), indicate that the reduction in Pd XPS intensity is not caused by an enlargement of the Pd particle size but, most probably, because of a decrease in the concentration of Pd in the top few nanometers of the external surface. This would confirm the confinement of Pd particles within the CTF structure.

Catalyst	Pd content [at%]	Elemental analysis [%]			Pd ⁰ [%]	Pd ^{δ+} [%]
		C	N	O		
Pd _{PVA} /CTF	3.0	63.8	7.0	26.2	65	35
Pd ^{II} _{IMP} /CTF	0.2	83.1	10.2	6.5	0	100
Pd _{IMP} /CTF	0.2	83.8	9.7	6.3	0	100
Pd _{IMP} /CTF after reaction	0.3	73.2	6.4	20.1	60	40

Further analysis of the Pd XPS data revealed interesting trends in the Pd oxidation states. Indeed, exposure to air was expected to produce partially oxidized Pd species, which happens in the case of the Pd_{PVA} material in which 35% of the Pd was oxidized (binding energy = 338.1 eV; Table 2).

Based on binding energies of known oxides, this Pd is consistent with Pd⁴⁺. Nevertheless, care should be taken in the interpretation of this data because of the difficulty to identify oxidation states of Pd with aromatic ligands,^[5,6] such as the CTF, formally because of electron-transfer effects with the ligands or because of initial/final state effects that influence the interpretation of XPS spectra of NPs.^[7]

For this reason, we will describe the Pd as Pd^{δ+} (Table 2). The remaining Pd was consistent with metallic Pd particles (binding energy = 335.8 eV; Figure 2 top). Surprisingly, we found only oxidized Pd in the Pd_{IMP}/CTF sample (Figure 2 bottom) as in the sample not yet reduced with NaBH₄ (Pd^{II}_{IMP}/CTF) (Figure 2 middle; binding energy = 388.1 eV). If re-oxidation occurred, we would expect the XPS data to be similar to that of the Pd_{PVA} samples because of the similar particle sizes, that is, a mixture of reduced and oxidized Pd. Therefore, we explored the possible diffusion limitation of the NaBH₄ reductant by the pore structure, which effectively shields the Pd^{δ+}, and analyzed the Pd^{δ+}_{IMP}/CTF after reduction with H₂. Again, there was no indication of reduced Pd. As there should be no diffusion limitation of H₂ during the reduction step, it is likely that the CTF network stabilizes the oxidized Pd. The presence of oxidized Pd in PdH_x would account for the XPS binding energy shifts observed and explain the insensitivity to H₂ reduction. It is likely that the stabilization of oxidized PdH_x species is enabled by the CTF.

High-resolution transmission electron microscopy (HRTEM) was performed to gain an insight into the structure and the composition of the Pd_{IMP}/CTF sample (Figure 3). HRTEM studies on over 100 Pd particles of the Pd_{IMP}/CTF catalyst revealed that most of the Pd particles have a face-centered cubic (fcc) structure with a unit cell parameter averaged at (4.01 ± 0.057) Å, which is considerably larger than that of pure metallic Pd (3.89 Å). It is known that deceptive lattice spacings could appear because of the complication of NPs that tilt randomly away from low-index-zone axis, particle shape effect, multiply twinned structures, etc., which could lead to a large deviation from the real lattice spacing and bending of the lattice planes in HRTEM. To avoid any possible misinterpretation of the expanded Pd lattice measured here, we selected the particles that exhibited a high contrast of lattices without lattice bend-

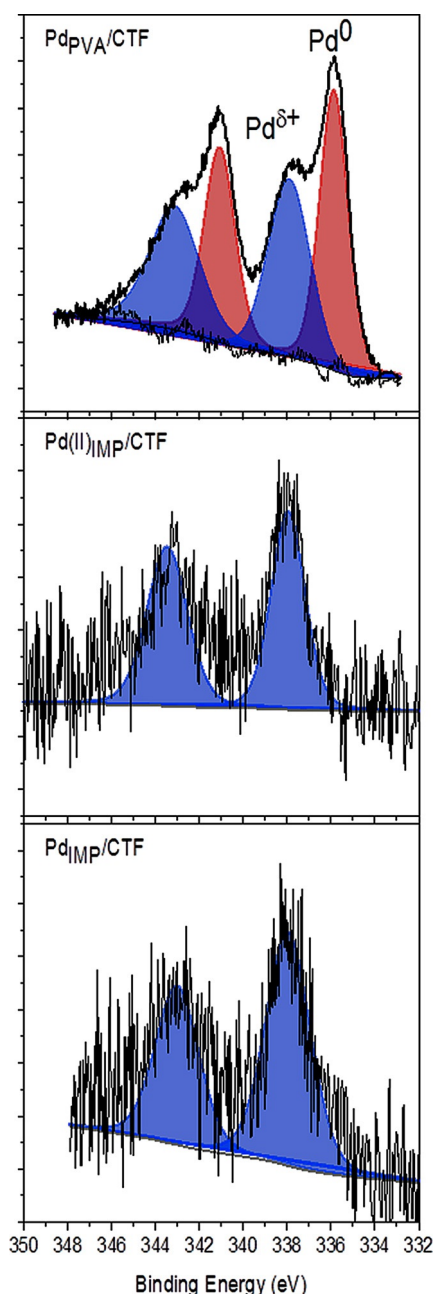


Figure 2. XPS data collected for Pd_{PVA} (top), Pd^{II}_{IMP} (middle), and reduced Pd_{IMP} (bottom). The low Pd_{IMP} signal is because Pd is incorporated within the CTF structure rather than confined on the outer surface of the CTF (Pd_{PVA}).

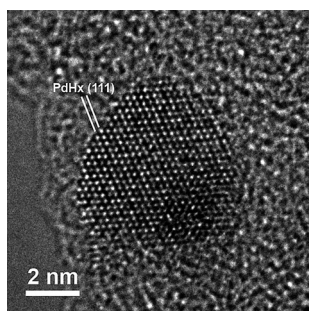


Figure 3. HRTEM image of Pd_{IMP}/CTF with enlarged (111) lattice spacing, which corresponds to a lattice parameter of 4.01 Å.

ing or abrupt shift carefully. The measured lattice spacings were derived by averaging at least seven consecutive lattice planes for each particle. According to the HRTEM simulation of the particles at different orientations, the variation of the Pd (111) lattice spacing should not exceed 1.2%, which is much smaller than the present case of $\approx 3\%$ expansion. Furthermore, more than 100 particles were measured for (111) or (200) lattice spacings and their random orientation should statistically minimize the deviation caused by crystal tilting. The measured lattice spacing value does not match any Pd oxide phase, but is identical to the lattice of PdH_x^[8] which suggests that H was introduced into the Pd lattices during the reduction treatment by NaBH₄. The presence of PdH_x ($x > 0-0.7$) species have been demonstrated after NaBH₄ treatment in the case of PdNPs embedded in Zr-modified mesoporous SiO₂ films.^[9] Furthermore, in situ heating of the Pd_{IMP}/CTF catalyst to 400 °C by using a Gatan heating holder in TEM led to a decrease of the lattice parameter to 3.94 Å, which was caused by the desorption of H. Similar results have been reported upon hydrogenation and dehydrogenation of a Pd film in environmental TEM.^[10]

Temperature-programmed (palladium) hydride decomposition (TPHD) experiments further confirm the presence of palladium hydrides stable under ambient conditions as appreciable hydrogen desorption occurs at low and high temperatures with onsets at 40 and 325 °C, respectively. Although the first hydrogen desorption peak occurs at PdH_x decomposition temperatures, typical of β -PdH in supported PdNPs,^[11] the second one occurs at an exceptionally high temperature. However, as a peak that parallels the onset and shape of the high temperature $m/z = 2$ peak is evident in the $m/z = 27$ signal (HCN), a partial decomposition of the CTF can occur. Thus, the hydrogen evolution can be attributed to Pd-catalyzed dehydrogenation.

The activity and selectivity of Pd/CTF catalysts were tested for the oxidation of glycerol. The reaction profiles obtained with Pd_{IMP}/CTF and Pd_{PVA}/CTF are compared in Figure 4. Pd_{IMP}/CTF, which contains only Pd^{δ+}, showed a surprisingly good catalytic activity, almost as good as that of Pd_{PVA}/CTF. The slight differences in activity cannot be attributed to a different particle size as TEM revealed a comparable size distribution in both cases.

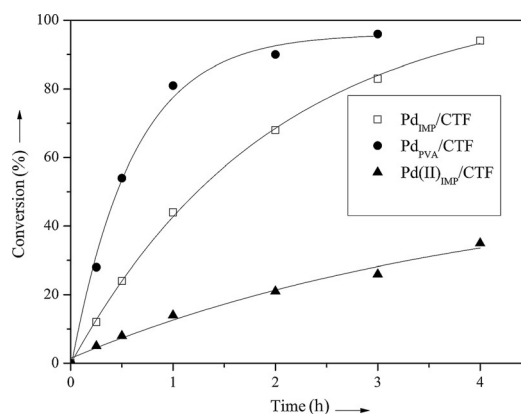


Figure 4. Reaction profiles for glycerol oxidation (0.3 M, NaOH/glycerol ratio = 4 mol/mol, glycerol/metal: 1000 mol/mol, 3 atm O₂, and 50 °C)

The lower activity of Pd_{IMP}/CTF than that of Pd_{PVA}/CTF could be attributed to the lower Pd exposure of the Pd_{IMP} sample, which is close to that reported for similar reactions.^[12,13] However, as noted previously, Pd_{IMP}/CTF appeared to contain significant concentrations of oxidized Pd. If the catalysts remained as Pd^{δ+}, there should be a significant decrease in activity as Pd^{II} is known to become active as an oxidation catalyst with oxygen under conditions harsher than those used in this study.^[14]

To identify the real nature and role of the Pd^{δ+} in the catalytic activity, Pd_{IMP}/CTF was tested before the reduction step, namely, Pd^{II}_{IMP}/CTF. The unreduced Pd^{II}_{IMP}/CTF showed a fairly good activity and reached 35% conversion after 4 h (Figure 4). These findings possibly suggested an in situ reduction of Pd inside the CTF framework. Indeed, XPS analysis of the used Pd_{IMP}/CTF confirmed the presence of ≈60% Pd⁰ (Table 2), which was likely produced from the reaction with glycerol or its reaction products.

In terms of selectivity, the Pd_{PVA}/CTF catalyst showed a higher selectivity to glyceric acid (81%) than Pd_{IMP}/CTF (62%; Table 3). The higher production of C₂ products in the case of

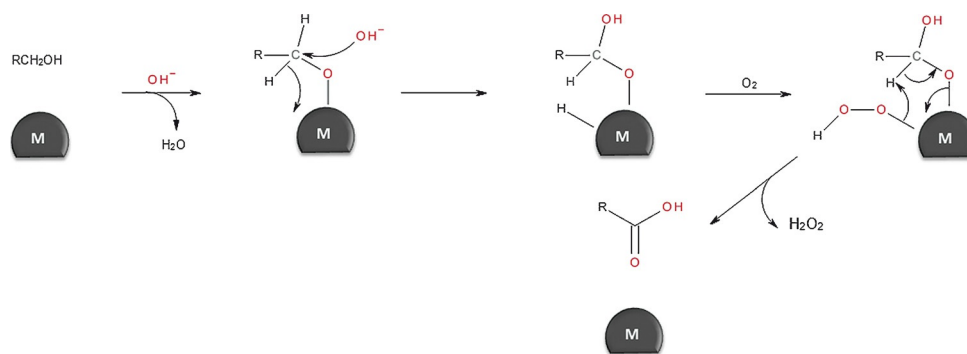
Catalyst	Selectivity at 90% conversion [%]			
	Glyceric acid	Glycolic acid	Oxalic acid	Tartronic acid
Pd _{PVA} /CTF	81	4	3	12
Pd _{IMP} /CTF	62	12	6	18

[a] Reaction conditions: 0.3 M, NaOH/glycerol ratio = 4 mol/mol, glycerol/metal: 1000 mol/mol, 3 atm O₂, 50 °C.

Pd_{IMP}/CTF compared to that of Pd_{PVA}/CTF cannot be justified in terms of the Pd particle size, which is similar (3.1 and 2.6 nm for Pd_{PVA}/CTF and Pd_{IMP}/CTF, respectively).

Therefore, the hydride particles in the Pd_{IMP}/CTF are likely to be responsible for the different selectivity of Pd_{IMP}/CTF with respect to Pd_{PVA}/CTF. If we consider the accepted reaction mechanism for glycerol oxidation (Scheme 1) in which a metal hydride is the intermediate formed, we could depict two different reaction pathways for PdH_x species: 1) the PdH_x could be transformed in situ by reaction with glycerol to form Pd⁰ and an oxidation product or 2) the PdH_x could reduce O₂ directly to generate H₂O₂ in higher concentrations than that generated during the first reaction step (Scheme 1).

As in situ H₂O₂ production is expected to promote C–C cleavage,^[15–17] this higher H₂O₂ local production would lead to a higher selectivity toward C–C cleavage products on Pd_{IMP}/CTF than that on Pd_{PVA}/CTF. Notably, in addition to the en-



Scheme 1. Accepted mechanism of metal-catalyzed glycerol oxidation.^[16b]

hanced H₂O₂ production, the desorption of the primary oxidation product (C₃ products) could be hindered because the reaction sites are located within the CTF structure, which would thus favor subsequent oxidation (i.e., C–C bond cleavage).^[18]

The evolution of the PdH_x species can be evaluated by recycling the catalyst, which also constitutes an important practical aspect. We compared the activity of Pd_{IMP}/CTF and Pd_{PVA}/CTF in a nine-run recycling test (Figure 5). The recycling tests were performed by simply filtering the catalyst and reusing it in the

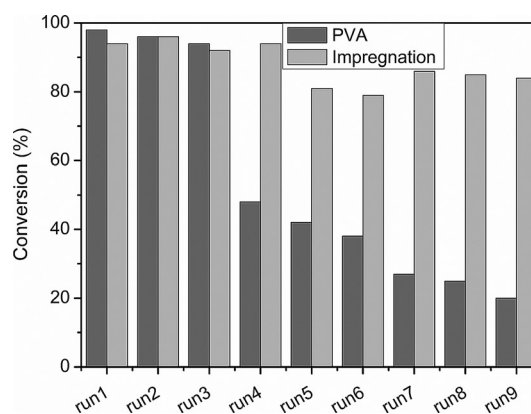


Figure 5. Conversion (4 h) of 1 wt% Pd_{PVA}/CTF and 1 wt% Pd_{IMP}/CTF upon recycling.

successive run without any further purification steps.^[2b] Pd_{IMP}/CTF showed very little deactivation (less than 5%) in nine subsequent runs (Figure 5) according to the physical/chemical stabilization expected to be provided by the embedding of the PdNPs inside the support framework. The small decrease of activity observed from the fifth run is attributed to the partial blocking of the active sites by adsorbed species. Indeed, XPS revealed a higher oxygen content in the used catalyst compared to the fresh one consistent with organic species trapped on the surface (Table 2).

After a single run, we also proved the absence of any catalytically active soluble specie by filtering the hot solution and letting the reaction proceed. No further conversion was observed in either case.

Furthermore, inductively coupled plasma (ICP) analysis showed that only 1% of the initial Pd amount was lost after nine runs. Conversely, under similar conditions, Pd_{PVA}/CTF showed a constant deactivation from the fourth run with a total Pd leaching of 6% (measured by ICP). The selectivity trend confirmed the transient presence of PdH_x that decreased during the reaction as highlighted by XPS. Indeed, the selectivity shown by Pd_{IMP}/CTF changed to become similar to that of Pd_{PVA}/CTF on recycling (Table 4).

Table 4. Selectivity to glyceric acid (S_{ga}) during the recycling of Pd_{IMP}/CTF (4 h reaction).

Runs	1	2	3	4	5	6	7	8	9
S_{ga} [%]	62	56	64	58	70	73	84	79	80

Conclusions

Herein, we demonstrated that the NaBH₄ reduction of Pd^{II} species inside a covalent triazine framework generates partly stable hydride species that have a significant effect on the selectivity in the liquid-phase oxidation of glycerol, which provides an indirect confirmation of the mechanism of glycerol oxidation in the presence of O₂ catalyzed by metal. From an application point of view, the physical confinement of Pd nanoparticles within the covalent triazine framework showed a beneficial effect on the durability of the catalyst.

Experimental Section

Materials

1,4-Dicyanobenzene (DCB) was purchased from Alfa Aesar and was used as received. Zinc chloride (Alfa Aesar, anhydrous, 98%) was stored in a glovebox and used as received. Na₂PdCl₄·2H₂O from Aldrich (99.99% purity), NaBH₄ of purity > 96% from Fluka, polyvinylalcohol (PVA; Mw = 13 000–23 000; 87–89% hydrolyzed) from Aldrich were used. Gaseous oxygen from SIAD was 99.99% pure.

Catalyst preparation

The support was prepared according to Ref. [1] by modifying the preparation as described by Chan-Thaw et al.^[2b] The monomer DCB and ZnCl₂, in a molar ratio of 1:5, were transferred into a quartz ampoule (3 × 12 cm) under an inert atmosphere. The ampoule was then evacuated, sealed, and heated within 30 min to 400 °C. After 20 h at 400 °C, the ampoule was further heated within 1 h to 600 °C and it was held for additional 20 h. The ampoule was then cooled to RT and opened. The resulting reaction mixture was washed several times with dilute HCl (0.1 M) under stirring to remove most of the ZnCl₂. The resulting black powder was washed with water until a neutral pH was obtained. After filtration, the material was dried at 150 °C and finely ground to give the CTF in a yield of 98%. The residual Zn content was checked by ICP, which resulted in a maximum amount of 0.3 wt%.

Sol immobilization

Pd sol: Na₂PdCl₄·2H₂O (0.043 mmol) and freshly prepared PVA solution (2 wt%, 880 μL) were added to water (130 mL). After 3 min, NaBH₄ solution (0.1 M, 860 μL) was added to the yellow-brown solution under vigorous magnetic stirring. The brown Pd⁰ sol was formed immediately. A UV/Vis spectrum of the Pd sol was recorded to ensure the complete reduction of Pd^{II}. Within few minutes of its generation, the suspension was acidified at pH 2 with sulfuric acid, and the support was added under vigorous stirring. The catalyst was collected by filtration and washed several times with distilled water. The samples were dried at 80 °C for 2 h. The amount of support was calculated to obtain a final metal loading of 1 wt%.

Impregnation

Na₂PdCl₄·2H₂O (0.235 mmol) diluted in water (20 mL) was added to the catalyst (0.5 g) and stirred vigorously for 6 h. NaBH₄ solution (Pd/NaBH₄ 1:16) was added to the solution, and it was stirred for 6 h. The catalyst was collected by filtration and washed several times to ensure the removal of the material that arose from the reduction treatment. The samples were dried at 80 °C for 2 h. The amount of support was calculated to obtain a final metal loading of 1 wt%. The obtained catalyst was labeled Pd_{IMP}/CTF.

Catalyst characterization

Morphology and microstructures of the catalysts were characterized by TEM. The powder samples of the catalysts were dispersed ultrasonically in ethanol and mounted onto copper grids covered with holey carbon film. A Philips CM200 LaB₆ electron microscope operated at 200 kV and equipped with a Gatan CCD camera was used for TEM observation. A FEI Titan 80–300 aberration-corrected electron microscope operated at 300 kV was used for HRTEM imaging.

ICP analysis was performed by using a Jobin Yvon JV24 to verify the quantitative metal loading on the support. The final total Pd loading was 1 wt%.

XPS data were collected by using a PHI 3056 spectrometer with an Al anode source operated at 15 kV and an applied power of 350 W. Samples were pressed manually between two pieces of In foil; the piece of In foil with the sample on it was then mounted on the sample holder with a piece of carbon tape (Nisshin E.M. Co. LTD). Adventitious carbon was used to calibrate the binding energy shifts of the sample (C 1s = 284.8 eV).^[19] High-resolution data were collected at a pass energy of 5.85 eV with 0.05 eV step sizes and a minimum of 200 scans to improve the signal-to-noise ratio; low-resolution survey scans were collected at a pass energy of 93.5 eV with 0.5 eV step sizes and a minimum of 25 scans.

TPHD was performed by using a home-made reaction rig. We placed 100 mg of sample in a Pyrex tubular reactor inserted in a furnace. The sample was heated under He flow (10 mL min⁻¹) at a rate of 10 °C min⁻¹. Decomposition products were detected by using a quadrupole MS (VGQ, Thermo electron Corporation) connected downstream. Hydrogen evolution was monitored by following the $m/z = 2$ signal, in addition the signals at $m/z = 12, 14, 16, 18, 26, 27, 28, 44, 45,$ and 77 were collected to reveal any eventual decomposition of the CTF material.

Catalytic test

The reactions were performed in a thermostatted glass reactor (30 mL) equipped with an electronically controlled magnetic stirrer connected to a large reservoir (5000 mL) that contained oxygen at 3 atm. The oxygen uptake was followed by using a mass flow controller connected to a PC through an A/D board, and we plotted flow versus time. Glycerol solution (0.3 M, NaOH/glycerol ratio = 4 mol/mol) and the catalyst (substrate/metal) 1000 mol/mol were mixed in distilled water (total volume 10 mL). The reactor was pressurized at the desired pressure of O₂ and thermostatted at 50 °C. The reaction was initiated by stirring. Samples were removed periodically and analyzed by HPLC using an Alltech OA-10308, 300 mm × 7.8 mm column and UV and refractive index (RI) detection to analyze the mixture of the samples. H₃PO₄ 0.1% solution was used as the eluent. The identification of the possible products was performed by comparison with the original samples.

Recycling tests

Each run was performed under the same conditions. The catalyst was recycled in the subsequent run after filtration without any further treatment using a fresh glycerol/NaOH solution.

Hot-filtration test

After the first run, the hot slurry (50 °C) was filtered to remove the catalyst, and the solution was stirred for an additional 1 h under O₂ pressure (3 atm).

Acknowledgements

We thank Phisan Katekomol for the preparation of the support. Financial support by the UniCat cluster of excellence (Unifying Concepts in Catalysis, Berlin) is gratefully acknowledged. A portion of this research was sponsored by the U.S. Department of Energy, Office of Basic Energy Sciences, Materials Sciences and Engineering Division (GMV). TEM characterization was performed at KIT and sponsored by Karlsruhe Nano Micro Facility (KNMF).

Keywords: cleavage reactions • heterogeneous catalysis • nitrogen heterocycles • oxidation • palladium

- [1] a) P. Kuhn, M. Antonietti, A. Thomas, *Angew. Chem. Int. Ed.* **2008**, *47*, 3450–3453; *Angew. Chem.* **2008**, *120*, 3499–3502; b) P. Kuhn, A. Forget, J. Hartmann, A. Thomas, M. Antonietti, *Adv. Mater.* **2009**, *21*, 897–901; c) A. Thomas, *Angew. Chem. Int. Ed.* **2010**, *49*, 8328–8344; *Angew. Chem.* **2010**, *122*, 8506–8523.
- [2] a) R. Palkovits, M. Antonietti, P. Kuhn, A. Thomas, F. Schüth, *Angew. Chem. Int. Ed.* **2009**, *48*, 6909–6912; *Angew. Chem.* **2009**, *121*, 7042–7045; b) C. E. Chan-Thaw, A. Villa, P. Katekomol, D. Su, A. Thomas, L. Prati, *Nano Lett.* **2010**, *10*, 537–541; c) C. E. Chan-Thaw, A. Villa, L. Prati, A. Thomas, *Chem. Eur. J.* **2011**, *17*, 1052–1057; d) C. E. Chan-Thaw, A. Villa, G. M. Veith, K. Kailasam, L. A. Adamczyk, R. R. Unocic, L. Prati, A. Thomas, *Chem. Asian J.* **2012**, *7*, 387–393.
- [3] T. Mallat, A. Baiker, *Catal. Today* **1994**, *19*, 247–283.
- [4] P. Kuhn, A. Forget, D. S. Su, A. Thomas, M. Antonietti, *J. Am. Chem. Soc.* **2008**, *130*, 13333–13337.
- [5] Z. M. Michalska, B. Ostaszewski, J. Zientarska, J. W. Sobczak, *J. Mol. Catal. A* **1998**, *129*, 207–218.
- [6] M. Heckenroth, E. Kluser, A. Neels, M. Albrecht, *Angew. Chem. Int. Ed.* **2007**, *46*, 6293–6296; *Angew. Chem.* **2007**, *119*, 6409–6412.
- [7] W. P. Zhou, A. Lewera, R. Larsen, R. I. Masel, P. S. Bagus, A. Wieckowski, *J. Phys. Chem. B* **2006**, *110*, 13393–13398.
- [8] W. Wunderlich, M. Tanemura in *Advances in Solid State Physics, Vol. 43* (Ed.: B. Kramer), Springer, **2003**, pp. 171–180.
- [9] a) J. Saha, A. Dandapat, G. De, *J. Mater. Chem.* **2011**, *21*, 11482–11485; b) M. Khanuja, B. R. Mehta, P. Agar, P. K. Kuriya, D. K. Avasthi, *J. Appl. Phys.* **2009**, *106*, 093515–093522.
- [10] T. Yokosawa, T. Alan, G. Pandraud, B. Dam, H. Zandbergen, *Ultramicroscopy* **2012**, *112*, 47–52.
- [11] M. Bonarowska, W. Raróg-Pilecka, Z. Karpinski, *Catal. Today* **2011**, *169*, 223–231.
- [12] S. Biella, F. Porta, L. Prati, M. Rossi, *Catal. Lett.* **2003**, *90*, 23–29.
- [13] A. Villa, A. Gaiassi, I. Rossetti, C. L. Bianchi, K. van Benthem, G. M. Veith, L. Prati, *J. Catal.* **2010**, *275*, 108–116.
- [14] a) B. P. Buffin, N. L. Belitz, S. L. Verbeke, *J. Mol. Catal. A* **2008**, *284*, 149–154; b) V. Jurčík, T. E. Schmid, Q. Dumont, A. M. Z. Slawin, C. S. J. Cazin, *Dalton Trans.* **2012**, *41*, 12619–12623; c) C. Melero, O. N. Shishilov, E. Álvarez, P. Palma, J. Cámpora, *Dalton Trans.* **2012**, *41*, 14087–14100.
- [15] W. C. Ketchie, Y. Fang, M. S. Wong, M. Murayama, R. J. Davis, *J. Catal.* **2007**, *250*, 94–101.
- [16] a) L. Prati, P. Spontoni, A. Gaiassi, *Top. Catal.* **2009**, *52*, 288–296; b) D. Wang, A. Villa, D. Su, L. Prati, R. Schlögl, *ChemCatChem* **2013**, *5*, 2717–2723.
- [17] M. Sankar, N. Dimitratos, D. W. Knight, A. F. Carley, R. Tiruvalam, C. J. Kiely, D. Thomas, G. J. Hutchings, *ChemSusChem* **2009**, *2*, 1145–1151.
- [18] A. Villa, C. E. Chan-Thaw, L. Prati, *Appl. Catal. B* **2010**, *96*, 541–547.
- [19] J. F. Moulder, W. F. Stickle, P. E. Solbol, K. D. Bomben, *Handbook of X-ray Photoelectron Spectroscopy*, PerkinElmer Corp., **1992**.

Received: January 21, 2015

Revised: March 2, 2015

Published online on June 26, 2015